14-3-3σ associates with cell surface aminopeptidase N in the regulation of matrix metalloproteinase-1

Abdi Ghaffari, Yunyaun Li, Ruhangiz T. Kilani and Aziz Ghahary*

Department of Surgery, BC Professional Firefighter's Burn and Wound Healing Research Laboratory, University of British Columbia, 344A JBRC, 2660 Oak Street, Vancouver, Canada, BC V6H 3Z6

*Author for correspondence (aghahary@interchange.ubc.ca)

Summary

Matrix metalloproteinases (MMPs) are implicated in the degradation of the extracellular matrix during development and tissue repair, as well as in pathological conditions such as tumor invasion and fibrosis. MMP expression by stromal cells is partly regulated by signals from the neighboring epithelial cells. Keratinocyte-releasable 14-3-3σ, or stratifin, acts as a potent MMP-1-stimulatory factor in fibroblasts. However, its mechanism of transmembrane signaling remains unknown. Ectodomain biotin labeling, serial affinity purification and mass spectroscopy analysis revealed that the stratifin associates with aminopeptidase N (APN), or CD13, at the cell surface. The transient knockdown of APN in fibroblasts eliminated the stratifin-mediated p38 MAP kinase activation and MMP-1 expression, implicating APN in a receptor-mediated transmembrane signaling event. Stratifin deletion studies implicated its C-terminus as a potential APN-binding site. Furthermore, the dephosphorylation of APN ectodomains reduced its binding affinity to the stratifin. The presence of a phosphorylated serine or threonine residue in APN has been implicated. Together, these findings provide evidence that APN is a novel cell surface receptor for stratifin and a potential target in the regulation of MMP-1 expression in epithelial–stromal cell communication.

Key words: 14-3-3 sigma, Aminopeptidase N, Matrix metalloproteinase, Signaling

Introduction

The complexity of multicellular organisms demands extensive communication between cells of different germ layers in order to direct tissue development and repair. Increasing evidence suggests that bidirectional signaling between stromal and epithelial cells plays a crucial role in maintaining the integrity of the extracellular matrix (ECM) and that a disruption in this communication can lead to fibrogenesis (Deitch et al., 1983; Machesney et al., 1998; Niessen et al., 2001) or predispose cells to malignancy (Bissell and Radisky, 2001; Radisky and Bissell, 2004). Matrix metalloproteinases (MMPs) represent a group of diverse proteolytic enzymes that are responsible for degradation of ECM and are involved in a variety of biological processes, such as tissue repair and remodeling, embryonic development, bone growth/resorption and tumor metastasis (Butler and Overall, 2009b; Nagase et al., 2006; Rodriguez et al., 2010). The synthesis of MMPs by stromal fibroblasts is partially regulated by neighboring epithelial cells primarily through diffusible cytokines and growth factors (Gabison et al., 2005; Garner, 1998; Harrison et al., 2006).

Stratifin (SFN, or 14-3-3σ) is a member of a large family of highly conserved 14-3-3 proteins, which are known to function as intracellular chaperones in signal transduction, apoptosis and cell cycle regulation (Hermeking, 2003; Pozuelo et al., 2004). Several groups have reported on the presence of 14-3-3 proteins in the extracellular space (Butler and Overall, 2009a; Katz and Taichman, 1999; Kobayashi et al., 2009; Leffers et al., 1993; Satoh et al., 1999). Our group has recently identified a novel function for the keratinocyte-releasable form of SFN as a potent MMP-1-stimulatory factor in dermal fibroblasts (Ghahary et al., 2004). It was found that SFN released from keratinocytes induces the expression of MMP1, MMP3, MMP8 and MMP24 in fibroblasts

through the p38 mitogen-activated protein kinase (MAPK) signaling pathway (Ghaffari et al., 2006; Ghahary et al., 2004; Lam et al., 2005). Furthermore, high levels of 14-3-3 eta (η) and gamma (γ) isoforms were detected in the synovial fluid of patients suffering from rheumatoid arthritis. The levels of 14-3-3η strongly correlated with the serum levels of MMP-1 and MMP-3, and the purified protein possessed MMP-1-stimulatory activity (Kilani et al., 2007).

The data presented indicate that releasable 14-3-3 might function as a ligand in a receptor-mediated transmembrane signaling pathway that leads to the induction of MMP-1 expression. Isoforms of 14-3-3 proteins have been reported to interact with the cytoplasmic domain of various plasma membrane proteins such as bullous pemphigoid antigen-2 or BP180 (Li et al., 2007), insulin-like growth factor I receptor (Craparo et al., 1997), muscle specific tyrosine kinase receptor (Strochlic et al., 2004), epidermal growth factor receptor (Oksvold et al., 2004) and type I transforming growth factor β receptor (McGonigle et al., 2001). However, no interaction between 14-3-3 proteins and the ectodomain of a cell surface receptor has been identified to date. In the current study, we report on the association between SFN and aminopeptidase N (APN) or CD13, a type 2 integral membrane protein, and highlight a transmembrane signaling mechanism for SFN-mediated MMP-1 expression in fibroblasts.

Results

rSFN exhibits cell surface binding activity

Human primary dermal fibroblasts, which are highly responsive to SFN activity (Ghahary et al., 2004), were used in a cell-binding assay to test the potential receptor binding activity of rSFN. To avoid nonspecific detection of intracellular 14-3-3 isoforms, a biotin-labeled recombinant rSFN (biotin–SFN) was prepared. Cells

were incubated with biotin–SFN at 4°C for 15 minutes and analyzed with fluorescent-conjugated streptavidin. The results revealed that biotin–SFN efficiently binds to the cell surface of fibroblasts (Fig. 1A, top panels). To ensure specific binding, the assay was repeated by competing biotin–SFN with an excessive amount of unlabeled rSFN. This nearly eliminated the binding activity of biotin–SFN (Fig. 1A, middle panels). The assay was also repeated with a biotin-labeled GST protein (biotin–GST) expressed by the same plasmid as rSFN (Ghahary et al., 2004). No cell binding activity was detected in the presence of biotin–GST (Fig. 1A, bottom panels). SFN binding to the cell surface was further evaluated by using a ^{125}I-labelled SFN (^{125}I-SFN) in a ligand–receptor binding assay. Cells treated with ^{125}I-SFN were incubated in the presence of an increasing concentration of unlabelled SFN for 2 h and then harvested by lysis buffer to measure the total binding in a gamma counter. As shown in Fig. 1B, more than 90% of the ^{125}I-SFN binding was replaced with competing and unlabelled SFN, demonstrating a specific SFN binding to the cell surface. A plasma membrane (PM) isolation technique was utilized to investigate the localization of the exogenous rSFN that had been added to the cells. Following a short incubation with biotin–SFN at 4°C, the PM and cytoplasmic fractions were separated by SDS-PAGE and analyzed by immunoblotting to identify biotin–SFN. As expected, biotin–SFN was detected predominantly in the membrane fraction (Fig. 1C). The GAPDH was not observed in the PM fraction, which indicated that the membrane preparation was devoid of cytosolic protein contamination. Exogenous biotin–GST was used in a separate group to control for the potential nonspecific binding of a biotin-labeled protein.

APN: a cell surface SFN receptor

To identify a candidate receptor for SFN, we employed a cell surface biotin labeling technique followed by serial SFN– and avidin–sepharose affinity purification. The ectodomains of PM proteins were labeled with a membrane-impermeable and non-cleavable biotin (sulfo-NHS–biotin), which binds covalently with the exposed primary amine groups. The cell membrane was disrupted by a mild lysis buffer and passed through an SFN– or blank-sepharose (control) batch column to isolate any potential SFN binding partners. To further purify potential candidates, the proteins retained by SFN–sepharose were eluted at acidic pH (glycine pH=2), neutralized and then passed through an immobilized avidin affinity column. Final purified proteins were eluted by the SDS sample buffer, separated by SDS-PAGE and visualized by sliver staining. As shown in Fig. 2A, silver staining of affinity-purified complex revealed several potential SFN-binding proteins. Streptavidin immunoblotting of the same sample identified two main biotinylated proteins at 170 and 150 kDa. As the 170 kDa band was also seen in the control group (blank sepharose), the 150 kDa protein was the only biotinylated membrane protein with binding affinity for SFN. To identify this protein, the SDS-PAGE band was subjected to trypsin digestion and liquid chromatography-mass spectrometry (LC–MS–MS) protein identification. The peptide sequences were analyzed with the MASCOT search engine. The peptides were aligned with the amino acids 485 to 498 and 843 to 855 of the human aminopeptidase N (APN) or CD13 (Fig. 2B). The probability-based Mowse score of 87 indicated a statistically significant alignment.

To confirm the results from the MS protein identification, we repeated the SFN–sepharose affinity binding using fibroblast cell lysates and separated the eluted complex by SDS-PAGE and subjected it to immunoblotting using an antibody against APN. Consistent with our original finding, the APN protein demonstrated a high binding affinity to immobilized SFN, as shown in Fig. 2C. To demonstrate further that rSFN is a specific binding partner for APN, we used membrane-impermeable bis-sulfosuccinimidyl suberate (BS[3]) to crosslink cell surface binding partners. Cells were incubated with rSFN before lysis and then crosslinked with BS[3]. Immunoblotting by the antibody against APN revealed a clear shift in the APN position only in the presence of rSFN and the BS[3] crosslinker (Fig. 2D). We also performed immunoprecipitation experiments with antibodies against each protein. Fibroblasts were incubated with rSFN, washed extensively and lysed before performing the immunoprecipitation. Two different antibodies against APN co-immunoprecipitated SFN, as detected by western blot analysis using an antibody against SFN (Fig. 2E, top panels).
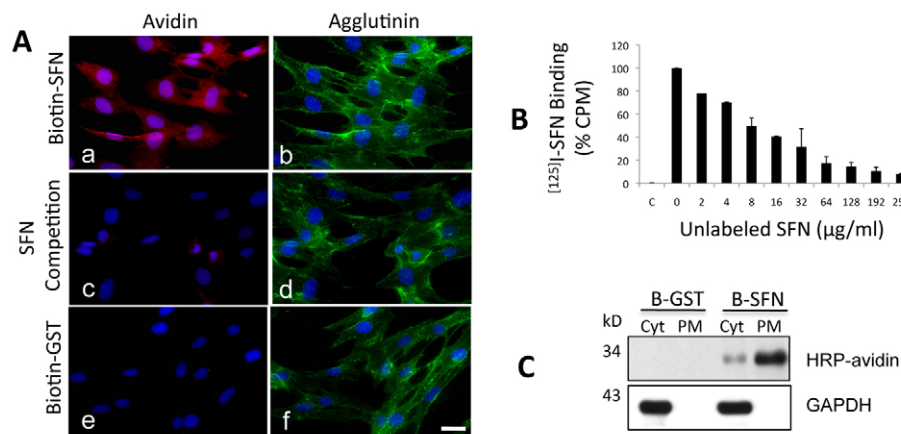

Fig. 1. rSFN cell surface binding activity. (**A**) Fibroblasts were treated with biotin–SFN in the absence (a,b) or presence of a 200-times excess of unlabeled rSFN (c,d), or biotin–GST as a negative control (e,f). Cells were then analyzed by immunofluorescence microscopy by anti-biotin streptavidin–alexa 568 or agglutinin–alexa 488 as a plasma membrane marker. (**B**) A receptor–ligand binding assay was performed by incubating cells with ^{125}I-labeled SFN in competition with an increasing concentration of unlabeled SFN. The radioactive count per minute (c.p.m.) is displayed as a percentage of ^{125}I-SFN binding in the absence of unlabeled SFN. (**C**) Plasma membrane (PM) and cytosolic (Cyt) fractions were isolated following incubation of cells with biotin–SFN (B-SFN) and biotin–GST (B-GST) and analyzed for the presence of biotin. GAPDH was used as a cytosolic marker to test the purity of the PM fraction. Scale bars: 20 μm.
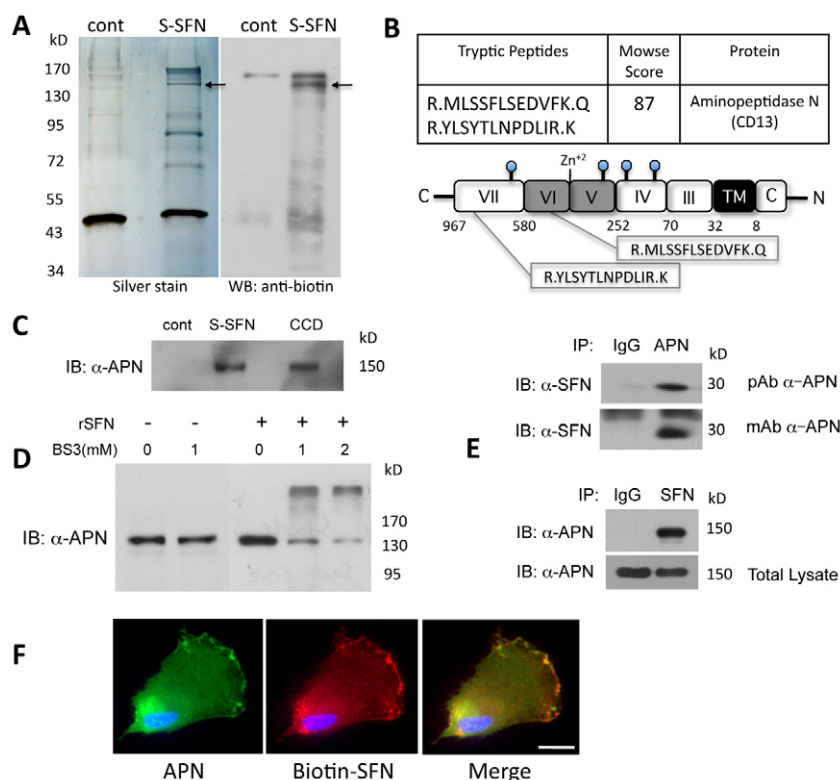
Fig. 2. Identification of the APN–SFN complex. (A) Silver stain and western blot of cell surface SFN-binding proteins isolated by serial affinity purification. The total cell lysate was initially passed through sepharose alone (Cont) or SFN–sepharose (S-SFN) before further purification by an avidin–agarose column. A 150-kDa biotin-labeled protein (arrow) was identified by western blot, and the equivalent band from the silver stain was subjected to trypsin digestion and mass spectroscopy (MS) analysis. **(B)** The alignment of the tryptic peptides, identified by MS sequencing, within the full APN sequence is shown. A Mowse score of 87 indicated a significant alignment by the MASCOT search engine. **(C)** Cell lysate was passed through a SFN–sepharose column, and the purified protein mixture immunoblotted with antibody against APN. An APN-expressing CCD-1064 cell lysate (CCD) was used as a positive control. **(D)** Cells were incubated with rSFN before treatment with 0, 1.0 or 2.0 mM BS^3 cross-linker. After separation of total lysate on SDS-PAGE, the shift in APN migration was revealed by immunoblotting. **(E)** Total cell lysates from rSFN-treated fibroblasts were immunoprecipitated (IP) with IgG or anti-APN polyclonal (pAb) and monoclonal (mAb) antibodies and immunoblotted with the antibody against SFN (top panels). The reverse IP by antibody against SFN pulled down APN from the total cell lysate (bottom panel). The level of APN in total cell lysate of both IgG and SFN IP groups is shown as the loading control. **(F)** A representative immunofluorescent image displaying the co-distribution of biotin–SFN and APN in fixed cells. Scale bar: 20 μm.

A reverse immunoprecipitation experiment further revealed that the antibody to SFN was able to co-precipitate APN protein, as shown in the lower panel of Fig. 2E. To study the co-distribution of APN and SFN, fixed cells were incubated with biotin–SFN at 4°C for 30 min before immunofluorescence analysis with a monoclonal antibody against APN and fluorescent-conjugated streptavidin. The representative image shown in Fig. 2, panel F, revealed a high level of co-distribution between biotin–SFN and APN at the leading edge of migrating fibroblasts. Cells that lacked an apparent leading edge (non-migrating) also displayed co-distribution between SFN and its receptor, although to a lesser extent (data not shown).

APN expression in vivo
To test the presence of the candidate SFN cell surface receptor in vivo, we examined the expression of APN and SFN in the normal and wounded rabbit ear by immunofluorescence. Dermal wound samples were collected on 16 days after injury, with a non-injured area in the back of the same ear used as a control. As expected, minimal expression of APN and SFN were observed in the uninjured skin (Fig. 3, panels a and c). However, examination of the wound revealed a large number of APN-positive cells throughout the dermis on day 16 post injury (Fig. 3, panel b), with the majority of the positive cells exhibiting a spindle-shaped fibroblast-like morphology. This coincided with an increase in the expression of SFN in the epidermis (Fig. 3, panel d), confirming the coexpression of the ligand in the wound. Immunofluorescence analysis of vimentin, a mesenchymal marker, was used to reveal that the majority of the cells in the dermis of the wounded skin exhibit a fibroblast phenotype (Fig. 3, insert in panel b). To study the co-distribution of SFN and its receptor in the skin at different stages of tissue repair, a longitudinal rat wound healing model was utilized, where tissue lysates from days 8, 11, 14, 17 and 30 post

wounding were analyzed by western blot. Although both SFN and APN were detected in the wound following re-epithelialization (day 11), there was a strong overlapping peak on day 30 post-wounding (Fig. 3, panel b). This provided evidence for the coexpression of this ligand and receptor during the remodeling phase of wound healing.

APN knockdown blocks SFN-mediated MMP-1 expression
Small interfering RNAs (siRNAs) were employed to knockdown APN expression in fibroblasts in order to examine the role of the APN–SFN interaction in SFN-mediated MMP-1 expression. Two different siRNA sequences were used against the mRNA encoding APN (GenBank accession number: NM_001150). Fig. 4A shows the inhibitory effect of siRNA on APN expression, as detected by immunofluorescence analysis. The quantification of the APN fluorescence intensity, which was normalized against the number of nuclei in each field (DAPI stain), revealed 50% and 80% inhibition at 10 and 50 nanomolar siRNA concentrations, respectively (Fig. 4A, right panel). The cells were then transfected with either non-silencing or APN siRNAs for 72 h and then treated with rSFN to examine the MMP-1 expression. The siRNA knockdown of APN sufficiently blocked the SFN-mediated MMP-1 expression, in contrast to the controls (Fig. 4B). The non-silencing siRNA concentration was matched with the highest dose of APN siRNA at 50 M. To exclude the possibility that APN siRNA would directly suppress MMP-1 expression, fibroblasts were treated with recombinant human interleukin-1 (rIL-1), a potent MMP-1-stimulatory cytokine (Mackay et al., 1992). As expected, the knockdown of APN by siRNA did not block the IL-1-mediated MMP-1 expression (Fig. 4C). In addition, we screened various strains of fibroblasts for expression of APN. IMR-90, a human fetal lung fibroblast, does not express APN protein at levels detectable by immunoblotting. Interestingly, IMR-90 was also the
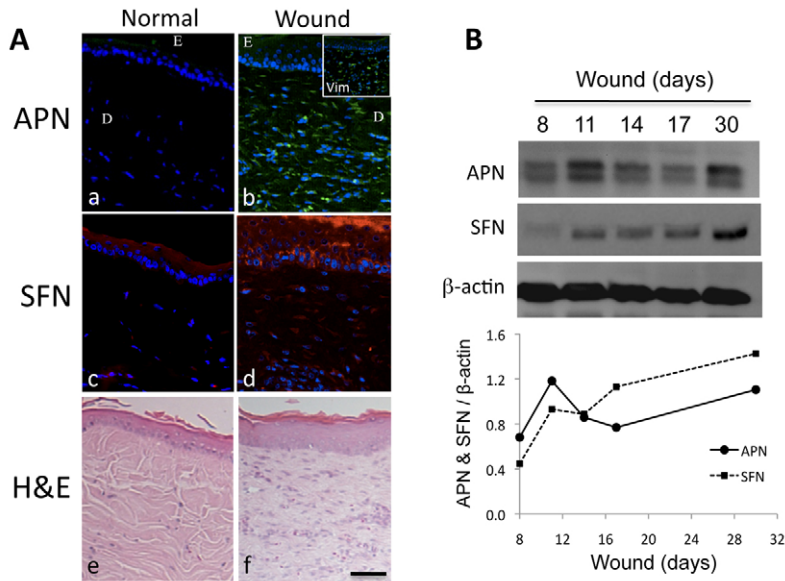
Fig. 3. APN expression in vivo. (A) Skin tissue samples were collected from the rabbit ear 16 days post injury and analyzed for APN (panel b) and SFN (panel d) expression by immunofluorescence microscopy. Uninjured tissue on the back of the same ear was used as a control (panels a and c). In the injured tissue (wound), APN was widely expressed in fibroblast-like cells in the dermis, confirmed by the expression of vimentin (Vim), as shown by the insert in panel b. Panels e and f represent the H&E stain of the sections shown in panels a and b, respectively. DAPI stain was used to mark the nucleus in panels a–d. E: epidermis; D: dermis. **(B)** In an in vivo full-thickness skin wound healing model, wound biopsies were obtained from five rats, using one animal at 8, 11, 14, 17 and 30 days post wounding. The protein levels of APN and SFN were determined in the total tissue lysate by western blotting. The level of β-actin was used as a loading control. To evaluate their co-distribution in tissue, the quantified expression of SFN and APN normalized against β-actin (by densitometry) is shown by the line graph in the lower panel. Scale bar: 50 μm.

only tested strain that was not responsive to SFN stimulation (Fig. 4D), even though these cells have been shown to express MMP-1 when stimulated by different collagen substrates (Abraham et al., 2007).

APN in SFN-mediated p38 MAPK activation

Previously, we have shown that stimulation with SFN leads to the transient activation of p38 MAPK (Lam et al., 2005). In the current study, we tested the intermediary role of APN in the activation of p38 by knocking down its expression before rSFN stimulation. The phosphorylation of p38 was analyzed by immunoblotting using a phospho-p38-specific antibody. Both non-transfected and control siRNA-transfected cells demonstrated phosphorylation of p38 following 90 min of stimulation by rSFN, whereas the APN knockdown significantly blocked the p38 activation by rSFN (Fig. 5). The relative APN and p-p38 levels from two separate experiments were quantified by densitometry analysis (Fig. 5, upper panel). This finding suggests that an interaction between SFN and APN is required to activate the p38 MAPK pathway and to induce MMP-1 expression in the dermal fibroblasts.

SFN–APN interaction

All 14-3-3 proteins, including SFN, comprise a dimerization region at the N-terminus as well as a target-binding region primarily concentrated at the C-terminus (Tzivion et al., 2001). To examine whether a specific region within SFN is responsible for its association with APN, a number of GST-fusion SFN fragments with deletions in the N- or C-termini were expressed in bacteria and purified with glutathione–sepharose (Fig. 6A, top panel). The binding capacity of APN with each GST–SFN fragment was then examined by a GST pulldown assay and analyzed by SDS-PAGE and western blot. The relative binding affinity of APN to each SFN fragment was quantified by densitometry analysis and normalized against the GST group (Fig. 6, panel A, bar graph). Deletions in the N-terminus (Nd50 and Nd100) did not affect the APN binding, in contrast to its binding with the full-sequence SFN. However, SFN fragments with 148 (Cd148) amino acid deletions from the C-terminus displayed a significant reduction in binding affinity to APN (Fig. 6A). Accordingly, the SFN MMP-1-stimulatory activity

was only diminished in the Cd148 deletion in contrast to the full length or Nd100 deletion (Fig. 6B). These findings suggest that the SFN C-terminus is the potential binding site for APN and the active site for MMP-1-stimulatory activity.

14-3-3 proteins regulate many cellular processes by binding to phosphorylated sites in target proteins (Pozuelo et al., 2004). We therefore tested the phosphorylation dependence of SFN binding to APN in the presence and absence of a phosphatase. Suspended intact cells were incubated with an alkaline phosphatase at 200 U/ml for 30 min at 30°C before lysis. Cell lysates of phosphatase-treated and control groups were then passed through a sepharose–SFN affinity column, and the APN level of the eluate was analyzed by western blotting. Surprisingly, the binding affinity of APN to SFN was significantly reduced following the dephosphorylation of the cell surface proteins (Fig. 6C, top left panel). As phosphorylation of APN has not been reported previously, we immunoprecipitated APN protein from primary fibroblasts before its separation by SDS-PAGE and western blot analysis. As shown in Fig. 6C (top-right panel), an antibody against phoshphoSer/Thr/Tyr clearly detected a band corresponding to the size of APN, demonstrating the presence of a phosphorylated amino acid residue in this protein. Immunoblotting also detected APN in the same blot at a molecular mass that matched the previously identified phosphorylated protein. In a separate experiment, live cells were incubated with phosphatase for 30 minutes at 37°C and then washed extensively before being treated with rSFN. A western blot analysis of MMP-1 expression revealed that the SFN-mediated upregulation of MMP-1 was attenuated in a dose-dependent manner as a result of pre-incubation with the phosphatase enzyme (Fig. 6C, lower panel). To rule out the indirect effect of dephosphorylation, the IL-1-mediated MMP-1 expression was shown to be unchanged in the presence of the phosphatase enzyme.

APN is a zinc-dependent metalloproteinase and a type II integral membrane ectoenzyme (Riemann et al., 1999). Bestatin is a potent inhibitor of APN enzymatic activity that blocks the active site by directly binding with the zinc ion (Addlagatta et al., 2006). To test the role of APN enzymatic activity in SFN-mediated MMP-1 expression, fibroblasts were pre-incubated with various doses of bestatin before treatment with rSFN. An APN enzymatic assay
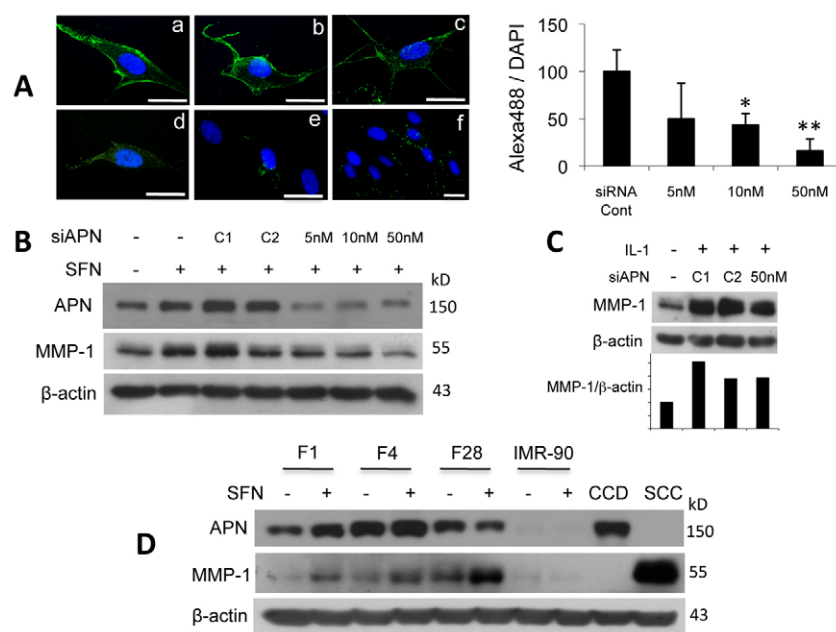
Fig. 4. APN knockdown blocks rSFN-mediated MMP-1 expression. (A) APN knockdown following siRNA transfection was quantified by immunofluorescence microscopy. The intensity of the APN immunofluorescence signal following transfection with (a) nothing, (b) nonsilencing siRNA, (c) 5 nM, (d) 10 nM and (e) 50 nM APN siRNA was quantified and normalized against the intensity of DAPI nucleus stain. At least five random fields were analyzed in each group. Transfection with 10 and 50 nM APN siRNA led to a 57% ($P<0.05$) and 84% ($P<0.001$) reduction of APN protein expression, respectively (graph). **(B)** Fibroblasts were transfected with an increasing dose of APN siRNA before treatment with rSFN and then analyzed for MMP-1 expression. For controls, cells were transfected with nothing (–), transfection buffer alone (C1) or nonsilencing siRNA (C2). **(C)** Fibroblasts were incubated with transfection buffer alone (C1), nonsilencing siRNA (C2) and 50 nM APN siRNA (siAPN) in the presence of rIL-1 and examined for the expression of MMP-1 (upper panel). The densitometry analysis of the same blots displays the ratio of MMP-1 to β-actin intensity. **(D)** APN and SFN-mediated MMP-1 expression levels were analyzed in primary human skin fibroblasts (F1, F4 and F28) as well as a human fetal lung fibroblast (IMR-90). IMR-90 was the only strain that did not express APN and was also non-responsive to SFN treatment. CCD-1064 cell (CCD) and squamous cell carcinoma (SCC) lysates were used as APN and MMP-1 positive controls, respectively. The level of β-actin was used as a loading control. Scale bars: 20 μm.

revealed a dose-dependent inhibition by bestatin in fibroblasts (Fig. 6D, upper panel). However, the bestatin had no effect on the SFN-mediated MMP-1 expression (Fig. 6D, lower panel). This finding suggests that APN enzymatic activity does not play a role in regulation of MMP-1 expression and that the enzyme active site is most likely not the binding site for SFN as the presence of bestatin did not block interaction with the ligand.

Discussion

The 14-3-3 proteins interact with over 200 binding partners and therefore regulate numerous cellular processes, mainly by inducing conformational changes in the target protein, masking of specific binding or active sites or the colocalization of two proteins (Yaffe, 2002). Although 14-3-3 proteins are mainly intracellular, their presence in the secretome of various cell lines (Butler and Overall, 2009a) as well as primary keratinocytes has been reported by others (Katz and Taichman, 1999; Leffers et al., 1993), followed by the unexpected discovery of their MMP-1-stimulatory activity by our group (Ghahary et al., 2004). It was recently suggested that, owing to a lack of conventional signaling peptide, keratinocyte-releasable SFN follows a non-classical secretory pathway involving the release of exosomes (Chavez-Munoz et al., 2008). In fact, several well-known extracellular proteins, including IL-1β and FGF-2, are also released by non-classical (ER/Golgi independent) pathways (Keller et al., 2008; Nickel, 2007). Activation of the p38 MAPK signal transduction pathway followed by a rapid increase in the expression of MMP-1 in response to SFN (Lam et al., 2005),

as well as its association with the cell surface of fibroblasts, all suggest the existence of a receptor-mediated transmembrane signaling pathway. In this study, biotin labeling of extracellular domains, serial affinity purification and LC–MS–MS protein sequencing have led us to identify APN or CD13 as a potential SFN cell surface receptor or co-receptor.

APN is an ectoenzyme metalloproteinase belonging to the M1 family and a type II integral membrane protein with a short N-terminal cytoplasmic domain. It is highly glycosylated, which contributes to at least 20% of its molecular mass. Furthermore, it is expressed in a wide variety of cells, such as myeloid cells, fibroblasts, renal and intestinal epithelia, and endothelial cells (Favaloro, 1991; Nomura et al., 2004; Riemann et al., 1999). APN has been referred to as a 'moonlighting' protein owing to its wide range of functions, such as the enzymatic regulation of peptides, viral receptor, tumor-homing peptide receptor, tumor cell invasion, proliferation and apoptosis, motility, antigen presentation, cholesterol uptake and signal transduction (Mina-Osorio, 2008). Our findings introduce a novel function for APN as a cell surface receptor for the SFN ligand, with a link to the signal transduction events leading to MMP-1 expression in fibroblasts. It will be interesting to see whether the interaction between APN and SFN also plays a role in the previously identified functions of APN in fibroblasts and other human cells.

The transmission of extracellular signals to MMP-1 gene expression in various cell types is mainly mediated by the family of serine/threonine-specific MAPKs, including ERK1/2 and p38
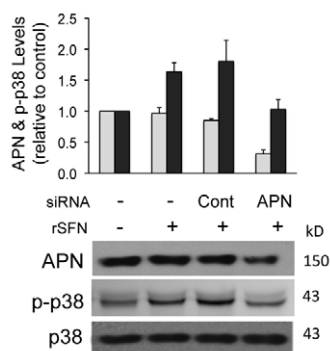
Fig. 5. APN knockdown blocks SFN-mediated p38 activation. Fibroblasts were transfected with non-silencing (cont) and APN siRNA (APN) before stimulation with rSFN and analyzed by western blot against total p38 MAPK (p38) and the phosphorylated form of p38 (p-p38). The relative intensities of APN (open bar) and p-p38 (solid bar) proteins were quantified by densitometry (top panel). The expression level of both proteins was normalized against the control (lane 1) in the absence of siRNA and rSFN.

MAPK subgroups (Nagase and Woessner, 1999). SFN stimulation of fibroblasts leads to a transient activation of p38 MAPK as well as an elevation in Jun and Fos – components of the heterodimeric AP-1 transcription factor – resulting in transcription of the gene encoding MMP-1 (Lam et al., 2005). Our findings indicate that APN knockdown is sufficient to block the p38 activation in the presence of an rSFN stimulus, suggesting a link between the APN and MAPK signaling cascade. In fact, signal transduction has been proposed as a mechanism of action for a number of APN functions that operate independently of its enzymatic activity (Mina-Osorio, 2008). Santos and colleagues found that the ligation of APN with monoclonal antibodies (mAbs) increases the intracellular free-calcium ions in monocytes and induces phosphorylation of ERK1/2, JNK and p38 MAPK. The same study also demonstrates that inhibitors of tyrosine kinases and phosphoinositide 3-kinase block the increase in calcium influx as well as the phosphorylation of MAPKs in the presence of the mAb against APN (Santos et al., 2000). In addition, antibodies to APN that have little effect on enzymatic activity exhibit a high capacity to induce cell adhesion in monocytes; this effect can be inhibited by SB203580, a p38 MAPK inhibitor (Mina-Osorio et al., 2006). APN has a very short cytoplasmic domain without any known signaling motifs (Luan and Xu, 2007). Therefore, it is possible that the APN interacts with a yet unidentified integral or peripheral signaling molecule in the SFN-mediated activation of p38 MAPK. In fact, Mina-Osorio and colleagues recently demonstrated the co-immunoprecipitation of Grb2 and Sos with APN from lysates of monocytic cells, suggesting a possible link between APN, Ras and the ERK1/2 MAPK signaling pathway (Mina-Osorio et al., 2006).
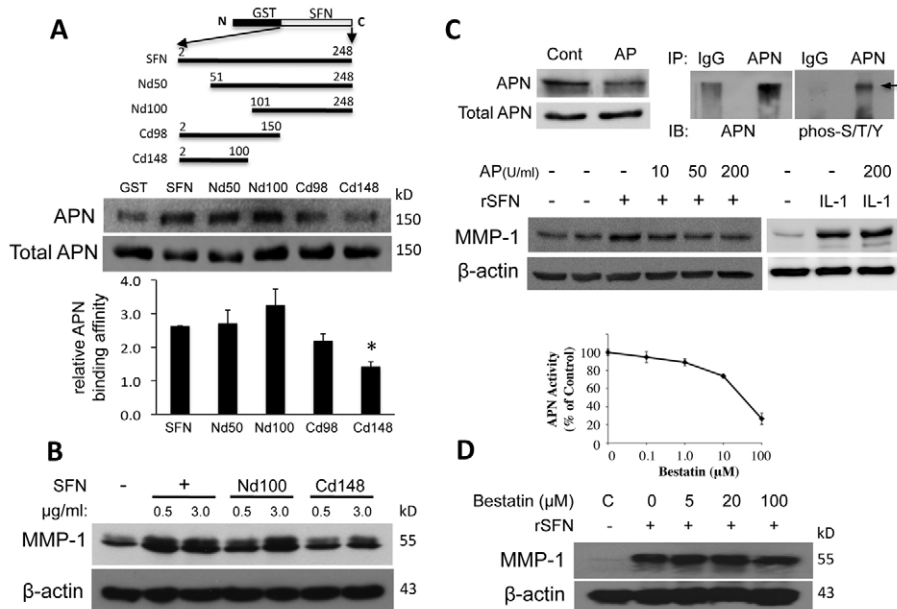

Fig. 6. The APN–SFN binding characteristics. (A) Deletion of the SFN C-terminus abrogates its binding capacity to APN. A schematic representation of various rSFN deletions fused with GST protein is shown at the top. The binding affinity of APN to each GST–rSFN fragment was analyzed by glutathione–sepharose affinity column purification and immunoblotting (bottom panel). GST–sepharose beads were used as the control (GST). The mean relative APN binding affinity to each SFN fragment was quantified by densitometry (N=2), as displayed in the bar graph. Nonparametric Kruskal–Wallis and Dunn's multiple comparisons tests revealed a significant difference (P≤0.05) between the SFN and Cd148 groups. The total APN in a small sample from each group is shown as the loading control. **(B)** The MMP-1-stimulatory activity of purified SFN, truncated Nd100 and Cd148 recombinant proteins was tested in fibroblasts. **(C)** Fibroblasts were incubated with alkaline phosphatase (AP) at 200 U/ml for 30 minutes, and the cell lysate was then subjected to an SFN affinity column and western blot to analyze APN–SFN binding (top left panel). To test for phosphorylation of APN, IgG or APN, immunoprecipitates from fibroblasts were separated by 7% SDS-PAGE. Immunoblotting with anti-phosphoSer/Thr/Tyr antibody detected a band corresponding to the size of APN (arrow). The same blot was used to immunoblot with antibody against APN (top-right panel). In a separate experiment, cells were incubated with an increasing concentration of the phosphatase (10, 50, 200 U/ml) before analysis of SFN-mediated MMP-1 expression (bottom panel). IL-1-mediated MMP-1 expression was also observed in the presence of 200 U/ml of phosphatase enzyme to evaluate the indirect effect of dephosphorylation on MMP-1 levels. **(D)** Blocking the APN enzyme active site did not inhibit the SFN-mediated MMP-1 expression. Bestatin inhibitory activity was first tested by an APN enzymatic assay (top panel). Cells were then incubated with various concentrations of bestatin (0, 5, 20, 100 μM) for 1 h before treatment with rSFN and analyzed for MMP-1 expression (lower panel).
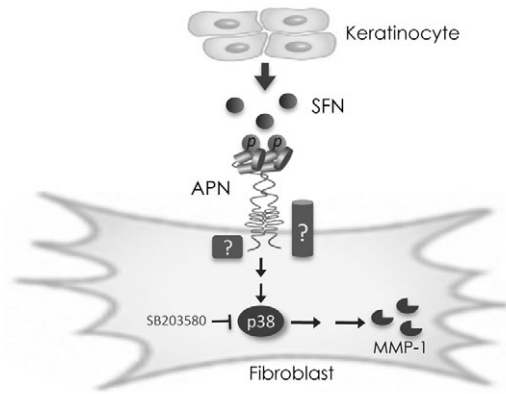
Fig. 7. The proposed role of APN in the SFN-mediated MMP-1 signaling pathway. Owing to possession of a short cytoplasmic domain, it is hypothesized that APN either acts as a co-receptor or binds with a peripheral plasma membrane signaling molecule before the activation of the p38 MAPK pathway and MMP-1 expression.

The co-distribution of SFN with APN at the leading edge of fibroblasts was unpredicted. Interestingly, an in vitro wound scratch assay revealed higher expression of APN within the migratory fibroblasts, where it co-distributed with vinculin, a migration marker (Lai et al., 2010). In addition, the inhibition of cell migration by reducing or blocking APN levels in tumor cells, lymphocytes and endothelial cells has also been reported (Terauchi et al., 2007; Proost et al., 2007). Therefore, the higher expression of APN receptor at the leading edge of migratory cells could explain the enhanced co-distribution results observed with biotin–SFN. Furthermore, the movement of cells through ECM is highly dependent on the activity of proteases such as MMPs (Gianneli et al., 1997; Kessenbrock et al., 2010; Pilcher et al., 1997; Pirila et al., 2003). This raises the possibility that SFN interaction with APN and the subsequent increase in MMP-1 activity could play a role in the cell migration of fibroblasts.

Our finding regarding the phosphorylation-dependent nature of SFN and APN binding is unexpected, mainly because APN is a type II plasma membrane protein with no previously reported phosphorylation sites. Nevertheless, a short incubation with a phosphatase is sufficient to block not only the binding between SFN and APN but also the expression of SFN-mediated MMP-1. An indirect effect on the signal transduction pathways was ruled out, as IL-1-mediated MMP-1 expression was not hindered by dephosphorylation of intact cells. Reports show that ECM proteins (osteopontin, sialoprotein, dentin matrix protein-1, phosphophoryn) as well as many secretory proteins (casein, enkephalin precursor, progastrin, chromogranin) become phosphorylated during their movement through the secretory pathway (Boskey et al., 2008; Turner et al., 1993). In addition, the extracellular phosphorylation of the ectodomains of integral proteins is not unprecedented. It has been shown that the CD36 ectodomain, a membrane receptor for thrombospondin and collagen, is phosphorylated by protein kinase C (PKC) (Asch et al., 1993). Ehrlich and Redegeld have also argued for the presence of adenosine triphosphate (ATP) and ectoprotein kinases in the extracellular space (Ehrlich et al., 1990; Redegeld et al., 1997). Although the detection of a phosphoSer/Thr/Tyr band points towards the existence of phosphorylated APN, this finding is still in its preliminary stages. Further work is under way to identify the exact phosphorylation

site(s) in APN by mass spectroscopy analysis and to investigate its role in SFN activity by site-directed mutagenesis.

Seven mammalian isoforms of 14-3-3 proteins have been described previously, all of which form dimers that bind to high-affinity phosphorylation-dependent motifs R[S/x]x(P)SxP and Rxxx(P)SxP (Yaffe et al., 1997) as well as to atypical phosphorylated and unmodified proteins (Fuglsang et al., 1999; Furlanetto et al., 1997; Waterman et al., 1998). All 14-3-3 proteins comprise a dimerization region located at the N-terminus and a target-protein-binding region located primarily in the C-terminus (Tzivion et al., 2001; Wang et al., 1999). The fragmentation study presented here reveals attenuation in the APN binding affinity following deletions in the SFN C-terminus, which indicates a potential binding site for APN. The effect of dimerization of 14-3-3 proteins on binding to a target protein seems to be dependent on the strength of their binding affinity. It has been shown that partners with high-affinity binding sites are able to bind to 14-3-3 even in the absence of dimerization (Tzivion et al., 1998; Yaffe et al., 1997). Interestingly, the deletions in the SFN dimerization interface (N-terminus) did not appear to affect its APN binding affinity in our study. This could indicate the presence of a high-affinity binding site within the extracellular domain of APN, allowing it to interact with the SFN monomer that lacks the N-terminal dimerization region.

The degradation of ECM by collagenases (e.g. MMP-1) is an essential component of pathophysiological events such as wound repair and tumor invasion. In wound repair, a significant portion of MMP production is performed by stromal fibroblasts, partly under the paracrine influence of local epithelial and immune cells (Toriseva and Kahari, 2009). Although the exact nature of APN and SFN interaction in wound healing remains unknown, we show an apparent co-distribution of SFN and APN in both the rabbit and rat tissue during the healing process. The rise in their expression appears to take place following re-epithelialization and during the early stages of the remodeling phase, where MMPs play a significant role in reorganization of the newly deposited granulation tissue.

APN or CD13, in combination with CD34 and collagen, is used as a cell surface marker in the identification of fibrocytes. Fibrocytes are peripheral blood-borne fibroblast-like cells that rapidly enter the injured site and synthesize ECM (Abe et al., 2001; Bucala et al., 1994). However, Sorrell and colleagues have demonstrated that the frequency and distribution of these cells do not account for the APN pattern in adult skin, indicating that fibroblasts could serve as another potential source of APN (Sorrell et al., 2003). In line with our in vivo findings, Mori and colleagues demonstrated an increase in the APN levels in the wounded versus uninjured skin of balb/c mice (Mori et al., 2005). This effect might be attributed to the reported APN enzymatic activity in ECM degradation (Saiki et al., 1993) or the role of APN in cellular motility and migration (Chang et al., 2005; Fukasawa et al., 2006). Based on our findings, it is also reasonable to speculate that the increased expression of APN is a response that augments cellular sensitivity to MMP-stimulating factors such as keratinocyte-derived SFN.

In cancer, it is the neighboring stromal fibroblasts in addition to malignant epithelial cells that contribute to the repertoire of MMPs responsible for the proteolytic breakdown of the peritumoral ECM (Egeblad and Werb, 2002; Overall and Lopez-Otin, 2002). Furthermore, stromal cells in tumors appear to be activated by paracrine factors released from malignant epithelial cells (Mueller

and Fusenig, 2004). Cell surface APN has been found to play a crucial role in tumor cell metastasis and is overexpressed in a wide range of solid tumors (Luan and Xu, 2007). Interestingly, an immunohistochemical examination of human lung carcinoma tissue revealed that the majority of APN-positive cells were in fact stromal fibroblasts (Ichimura et al., 2006). It is therefore tempting to speculate that epithelial-released factors such as SFN can act through the APN receptor to induce MMP production by neighboring stromal fibroblasts. If this hypothesis is correct, then the reported increases in expression of both APN and MMPs in the tumor microenvironment are connected events and not simply a coincidence. In fact, new data from our laboratory show a significant increase in the expression of APN by fibroblasts when co-cultured with keratinocytes or treated with keratinocyte-derived conditioned medium (Lai et al., 2010).

In conclusion, the data presented in this paper identify APN as a novel cell surface receptor for the SFN ligand and enable us to propose a new function for this type II integral membrane protein in the SFN-mediated activation of p38 MAPK and MMP-1 expression in fibroblasts. As indicated in Fig. 7, our findings also raise a few key questions about the exact mechanism of APN activation by SFN. Does APN act alone or as a co-receptor? Where is the SFN binding site on the APN ectodomain? Where exactly are the phosphorylation sites on APN? Answers to these questions could pave the way for targeting APN in the treatment of disorders marked by an imbalance in MMP expression.

Materials and Methods
Cell culture and reagents
Following informed consent, foreskin samples were obtained from patients undergoing elective surgery under local anesthesia. Written informed consent was obtained from each participant, and the study was approved by the University of British Columbia Hospital Human Ethics Committee and conducted according to the Declaration of Helsinki Principles. Human primary dermal fibroblasts were harvested as described previously (Ghaffari et al., 2006). Fibroblasts, balb/3T3 and 293T cells were grown in DMEM supplemented with 10% fetal bovine serum (FBS) and antibiotic-antimycotic preparation (100 U/ml penicillin, 100 µg/ml streptomycin and 0.25 µg/ml amphotericin B). The human fetal lung fibroblast cell line IMR-90 (ATCC, Manassas, VA) was cultured in DMEM plus 10% FBS. The CCD-1064Sk cell lysate (Santa Cruz Biotechnology, Santa Cruz, CA) was used as a positive control for APN protein expression. Calf intestinal alkaline phosphatase (AP) (New England Biolabs, Ipswich, MA) was used for the protein dephosphorylation experiment according to the manufacturer's instructions. Bestatin hydrochloride (Sigma Chemicals, Oakville, ON, Canada) was used as a competitive and specific inhibitor of APN enzymatic activity. Cell lines isolated from human squamous cell carcinoma (SCC) were obtained from the American Type Culture Collection (ATCC, Manassas, VA) and used as positive controls for MMP-1 expression.

Recombinant protein expression
Expression vectors for human stratifin have been described previously (Li et al., 2007). In brief, the human gene encoding full-length stratifin was subcloned into prokaryotic expression vectors pGEX-6P-1 (GE Healthcare Bio-Sciences, Quebec, Canada) and pET-28a(+) (Novagen, Madison, WI) for fusion protein tagged with glutathione S-transferase (GST) and histidine (His), respectively. The His-tagged SFN was purified using a Ni-Sepharose column according to the manufacturer's instructions (GE Healthcare Bio-Sciences, Quebec, Canada). Different fragments of SFN fused to GST were also prepared as described previously (Li et al., 2007). Fusion proteins containing peptide fragments of SFN were referred to as Nd50 (amino acids 51–246), Nd100 (amino acids 101–246), Cd98 (amino acids 1–150) and Cd148 (amino acids 1–100). GST-tagged SFN fragments bound to glutathione-sepharose (GE Healthcare Bio-Sciences, Quebec, Canada) were then used in affinity binding experiments.

Cell and ligand binding assays
To examine the cell binding activity of SFN protein, 5×10^4 primary human fibroblasts were plated in a 12-well plate on a glass coverslip overnight. The cells were then serum starved for 3 h before the addition of protein. Recombinant stratifin (rSFN) in PBS was labeled with Sulfo-NHS-LC-Biotin (Pierce, Rockford, IL) in a 3:1 ratio (Biotin:rSFN), as instructed by the manufacturer. Cells were blocked with 1.0% bovine serum albumin (BSA) in DMEM for 30 minutes before the addition of biotin–SFN at 1.0 µg/ml for 15 minutes at 4°C and then washed extensively with

PBS. Biotin-labeled glutathione S-transferase (biotin–GST) was used as a negative control. The competition assay was performed by pre-incubating cells with 200 µg/ml of rSFN for 30 minutes at 4°C before adding biotin–SFN. Biotin was detected by immunofluorescence microscopy using streptavidin–alexa 568 (Invitrogen, Eugene, OR). To perform a ligand–receptor binding assay, rSFN was labeled with ^{125}I (New England Nuclear, Boston, MA) and Iodo-Gen reagent (Pierce, Rockford, Illinois) according to the manufacturer's instructions and as described previously (Uludag et al., 1999). Following a wash with cold PBS, fibroblasts were incubated with ^{125}I-SFN (5×10^5 c.p.m.) in the absence and presence of an increasing concentration of unlabeled rSFN for 2 h at 4°C. Unincorporated radiolabel was then washed out with cold PBS, the cells were harvested by lysis buffer and the total binding of radiolabel was measured in a liquid scintillation counter (Beckman coulter, Mississauga, ON, Canada).

Collection of cell lysate and fractions
For total cell lysates, following an extensive wash with PBS, cells were disrupted in lysis buffer [50 mM Tris-HCl, 150 mM NaCl, 1.0 mM EDTA, 1.0 mM EGTA, 0.025% NaN$_3$, 1% Triton X-100, 0.5% IGEPAL, protease inhibitor cocktail (Sigma Chemicals, Oakville, ON, Canada), at pH 7.5] and centrifuged at 16,000 **g** for 15 min. For preparation of the cell fractions, cells were released by EDTA and collected in tissue disruption buffer (150 mM NaCl, 20 mM Na$_2$HPO$_4$, 2 mM NaH$_2$PO$_4$, 20% glycerol, 2 mM sodium orthovanadate and protease inhibitor cocktail) and homogenized in a Dounce homogenizer glass (Fisher, Ottawa, ON, Canada). Homogenized preparations were further disrupted by sonication on ice and then centrifuged at 19,000 **g** to remove nuclei and cell debris. The supernatant was then centrifuged at 100,000 **g** for 90 minutes at 4°C. The soluble cytoplasmic fraction (supernatant) was collected, and the remaining pellet (total membrane fraction) was solubilized in lysis buffer.

Purification of cell surface stratifin-binding proteins
Following release of fibroblasts with EDTA, cell surface proteins of intact cells were biotinylated using 2 mM water-soluble and membrane-impermeable EZ-Link sulfo-NHS-LC-biotin reagent (Pierce, Rockford, IL) in PBS for 30 minutes at 4°C. Free biotin was quenched and removed by three washes of cold PBS plus 100 mM glycine. To obtain the total cell lysate, cells were disrupted in lysis buffer (50 mM Tris-HCl; 10 mM EDTA; 5 mM EGTA; 0.025% NaN$_3$; 1% Triton-X100; 0.5% IGEPAL CA-630; protease inhibitor) for 30 minutes by gentle rotation at 4°C and then cleared by centrifugation at 18,000 **g** for 10 min at 4°C. Affinity-purified His–SFN was dialyzed against PBS and then conjugated with CNBR-activated Sepharose 4B (GE Healthcare Bio-Sciences, Quebec, Canada) at a ratio of 10 µmole ligand to 1.0 ml of sepharose, according to the manufacturer's instructions. A deactivated and blank Sepharose-4B was used as a control. Biotin-labeled cell lysate was then applied to a 30 µl bed of sepharose–SFN or sepharose alone for 2 h at 4°C with gentle rotation. Beads were then washed seven times with PBS plus 1% Tween-20, eluted with 100 mM glycine at pH 2.0. The glycine sample was neutralized with 1 M Tris solution, applied to 30 µl of Avidin–Agarose (Sigma-Aldrich, Oakville, ON, Canada) for 1 h at 4°C and washed three times with PBS plus 1% Tween-20. Biotinylated proteins were then eluted by SDS loading buffer [0.35 M Tris-HCl, 10.28% (w/v) SDS, 36% (v/v) glycerol, 5% 2-mercaptoethanol, 0.012% (w/v) bromophenol blue] with a 10 min incubation at room temperature followed by a 5 min boil. Eluted proteins were resolved by 10% precast keratin-free SDS-PAGE (Bio-Rad, Hercules, CA) and either immunoblotted with streptavidin-HRP or stained with ProteoSilver silver (Sigma-Aldrich, Oakville, ON, Canada). For protein sequencing, purified biotinylated proteins excised from silver-stained gels were subjected to trypsin digestion and identified by API Q STAR PULSARi Hybrid LC–MS–MS at the University of British Columbia MSL/LMB Proteomics Core Facility. The peptide sequences were analyzed using the Mascot search engine and Analyst software (Applied Biosystems, Foster City, CA) against the non-redundant NCBI database.

Western blotting
Cell lysates, cell fractions or purified proteins were transferred to PVDF membrane with Mini Trans-Blot Cell (Bio-Rad, Hercules, CA) after separation by SDS-PAGE. Immunoblotting was carried out with the following the antibodies: 1:5000 streptavidin–HRP (Pierce, Rockford, IL); 1:5000 anti-GAPDH (R&D Systems, Minneapolis, MN); 1:500 anti-APN [3D8] (Santa Cruz Biotechnology, Santa Cruz, CA); 1:1000 anti-stratifin (Medicorp, Montreal, QC, Canada); 1:500 anti-MMP-1 (R&D Systems, Minneapolis, MN); 1:1000 anti-phosphoserine/threonine/tyrosine (Abcam, Cambridge, MA); 1:20,000 anti-β-actin (Sigma-Aldrich, Oakville, ON, Canada); 1:3000 anti-mouse IgG-HRP and anti-rabbit IgG-HRP (Bio-Rad, Hercules, CA). Protein bands were visualized by an ECL detection system (Santa Cruz Biotechnology, Santa Cruz, CA).

Immunoprecipitation
Fibroblasts were released by EDTA and washed with PBS before incubating with rSFN for 30 minutes at 4°C. Soluble cell lysate was collected in lysis buffer, cleared by centrifugation and immunoprecipitated by 2 µg/ml monoclonal anti-APN [3D8], 2 µg/ml polyclonal anti-APN [H300] (Santa Cruz Biotechnology, Santa Cruz, CA) or anti-SFN antibody at 4 µg/ml for 1 h at 4°C with gentle rotation. Non-immunized

rabbit and mouse IgG were used as controls. Immune complexes were collected on protein G–Sepharose beads (50 μl/ml) (GE Healthcare Bio-Sciences, Quebec, Canada) for 1 h at 4°C, washed five times with PBS.T (0.1% Tween-20), eluted by boiling in sample buffer and resolved by SDS-PAGE for western blot analysis.

siRNA knockdown of aminopeptidase N

APN protein knockdown was tested by two different siRNA oligonucleotide sequences: si_ANPEP_1, CCGAAATGCCACACTGGTCAA, and si-ANPEP_2, CCGGGTGAACTACGACGAAGA purchased from Qiagen (Valencia, CA). A non-silencing siRNA, with the same GC content as that of APN siRNA, conjugated with Alexa Fluor 488 was used as a control and for monitoring transfection by fluorescence microscopy. HiPerfect transfection reagent was used according to the manufacturer's recommendations (Qiagen). Proliferating fibroblasts were harvested and 1×10^5 cells plated in six-well dishes containing 5, 10 or 50 nM siRNA oligonucleotide. The medium was replaced 24 h post-transfection, and the cells were treated with rSFN (2.5 μg/ml) at 72 h post-transfection.

In vivo wound healing models

All animals were cared for in accordance with the guidelines of the Canadian Council on Animal Care and with approval from the University of British Columbia Animal Welfare and Policy Committee. Female New Zealand white rabbits weighing approximately 4–5 kg were used in the rabbit ear fibrotic wound model. After the rabbits were anaesthetized, 8-mm diameter full-thickness wounds down to the perichondrial membrane were created, as described previously (Lee et al., 2005; Morris et al., 1997). On day 16 post wounding, when reepithelialization was complete, the rabbits were euthanized and the wounds harvested and fixed in 2% PFA before embedding in paraffin. Normal and non-injured skin on the back of the same ear was used as the control. Sprague–Dawley rats were used as described previously in a longitudinal wound healing study to monitor levels of APN and SFN at different stages of dermal repair (Li et al., 2006). In brief, six full-thickness excisional wounds (6.0 mm diameter) were made on the dorsal surface of rat skin and allowed to heal for up to 30 days. One animal was euthanized on each post-wound day 8, 11, 14, 17 and 30, and a 4.0 mm punch biopsy was obtained from the injured area and frozen at –80°C. Tissue samples were weighed-out and homogenized in lysis buffer with a tissue homogenizer (Qiagen, Valencia, CA) and glass pestle, followed by sonication. A Bradford protein assay was performed, and an equal amount of tissue lysate (75 μg) was separated by SDS-PAGE, as described above. Tissue lysates from three random wounds were pulled together for this experiment.

Immunofluorescence microscopy

Cultured fibroblasts were grown on glass coverslips, fixed with 1% paraformaldehyde (PFA) for 15 min on ice and blocked with 2% BSA in PBS. For staining the plasma membrane, wheat germ agglutinin–Alexa 488 (Invitrogen, Eugene, OR) was added (1:2000 dilution) before fixing the cells. APN was detected using mouse anti-APN 3D8 antibody (Santa Cruz) followed by Alexa-488-conjugated goat anti-mouse IgG (Invitrogen, Eugene, OR). Biotin-labeled SFN was detected with Alexa-568-conjugated streptavidin (Invitrogen, Eugene, OR). To observe the APN protein expression in the normal and injured rabbit skin tissue, paraffin-embedded sections fixed in 2% PFA were incubated with a 1:50 dilution of 3D8 antibody against APN followed by goat anti-mouse Alexa 488 secondary antibody (1:2500 dilution). Samples were mounted in ProLong Gold antifade reagent with DAPI (Invitrogen, Eugene, OR) and examined by a Zeiss Axioplan-2 fluorescence microscope and Northern Eclipse image analysis software. A second tissue section was stained with haematoxylin and eosin (H&E) for histological analysis.

Enzymatic assay

The quantitative assays for APN on cultured human dermal fibroblasts were performed according to previously published methods (Raynaud et al., 1992). In brief, all assays were performed in triplicate using Ala-4 nitroanilide (Ala-pNA, Sigma-Aldrich, Oakville, ON, Canada) in phosphate buffer pH 7.4 as a chromogenic substrate. Ala-pNA (100 μl) was added at a concentration of 5 mM to 10^5 cells. Reactions were stopped by adding 900 μl acetate buffer (1.0 M, pH 4.4) after 60 min of incubation at 37°C. After centrifugation (2 min at 10,000 *g*), the absorbance of the supernatant was detected spectrophotometrically at 405 nm.

Statistical analysis

Data were expressed as means ± s.d. and analyzed with one-way analysis of variance with a Tukey–Kramer multiple comparison test among different groups where indicated. The comparisons of more than two groups with low sample size were carried out by nonparametric Kruskal–Wallis and Dunn's multiple comparisons tests. P-values less than 0.05 were considered statistically significant in this study. All experiments were repeated three times, unless indicated otherwise.

References

Abe, R., Donnelly, S. C., Peng, T., Bucala, R. and Metz, C. N. (2001). Peripheral blood fibrocytes: differentiation pathway and migration to wound sites. *J. Immunol.* **166**, 7556-7562.

Abraham, L. C., Dice, J. F., Lee, K. and Kaplan, D. L. (2007). Phagocytosis and remodeling of collagen matrices. *Exp. Cell Res.* **313**, 1045-1055.

Addlagatta, A., Gay, L. and Matthews, B. W. (2006). Structure of aminopeptidase N from Escherichia coli suggests a compartmentalized, gated active site. *Proc. Natl. Acad. Sci. USA* **103**, 13339-13344.

Asch, A. S., Liu, I., Briccetti, F. M., Barnwell, J. W., Kwakye-Berko, F., Dokun, A., Goldberger, J. and Pernambuco, M. (1993). Analysis of CD36 binding domains: ligand specificity controlled by dephosphorylation of an ectodomain. *Science* **262**, 1436-1440.

Bissell, M. J. and Radisky, D. (2001). Putting tumours in context. *Nat. Rev. Cancer* **1**, 46-54.

Boskey, A. L., Doty, S. B., Kudryashov, V., Mayer-Kuckuk, P., Roy, R. and Binderman, I. (2008). Modulation of extracellular matrix protein phosphorylation alters mineralization in differentiating chick limb-bud mesenchymal cell micromass cultures. *Bone* **42**, 1061-1071.

Bucala, R., Spiegel, L. A., Chesney, J., Hogan, M. and Cerami, A. (1994). Circulating fibrocytes define a new leukocyte subpopulation that mediates tissue repair. *Mol. Med.* **1**, 71-81.

Butler, G. S. and Overall, C. M. (2009a). Proteomic identification of multitasking proteins in unexpected locations complicates drug targeting. *Nat. Rev. Drug Discov.* **8**, 935-948.

Butler, G. S. and Overall, C. M. (2009b). Updated biological roles for matrix metalloproteinases and new "intracellular" substrates revealed by degradomics. *Biochemistry* **48**, 10830-10845.

Chang, Y. W., Chen, S. C., Cheng, E. C., Ko, Y. P., Lin, Y. C., Kao, Y. R., Tsay, Y. G., Yang, P. C., Wu, C. W. and Roffler, S. R. (2005). CD13 (aminopeptidase N) can associate with tumor-associated antigen L6 and enhance the motility of human lung cancer cells. *Int. J. Cancer* **116**, 243-252.

Chavez-Munoz, C., Morse, J., Kilani, R. and Ghahary, A. (2008). Primary human keratinocytes externalize stratifin protein via exosomes. *J. Cell. Biochem.* **104**, 2165-2173.

Craparo, A., Freund, R. and Gustafson, T. A. (1997). 14-3-3 (epsilon) interacts with the insulin-like growth factor I receptor and insulin receptor substrate I in a phosphoserine-dependent manner. *J. Biol. Chem.* **272**, 11663-11669.

Deitch, E. A., Wheelahan, T. M., Rose, M. P., Clothier, J. and Cotter, J. (1983). Hypertrophic burn scars: analysis of variables. *J. Trauma* **23**, 895-898.

Egeblad, M. and Werb, Z. (2002). New functions for the matrix metalloproteinases in cancer progression. *Nat. Rev. Cancer* **2**, 161-174.

Ehrlich, Y. H., Hogan, M. V., Pawlowska, Z., Naik, U. and Kornecki, E. (1990). Ectoprotein kinase in the regulation of cellular responsiveness to extracellular ATP. *Ann. NY Acad. Sci.* **603**, 401-416.

Favaloro, E. J. (1991). CD-13 ('gp150'; aminopeptidase-N): co-expression on endothelial and haemopoietic cells with conservation of functional activity. *Immunol. Cell Biol.* **69**, 253-260.

Fuglsang, A. T., Visconti, S., Drumm, K., Jahn, T., Stensballe, A., Mattei, B., Jensen, O. N., Aducci, P. and Palmgren, M. G. (1999). Binding of 14-3-3 protein to the plasma membrane H(+)-ATPase AHA2 involves the three C-terminal residues Tyr(946)-Thr-Val and requires phosphorylation of Thr(947). *J. Biol. Chem.* **274**, 36774-36780.

Fukasawa, K., Fujii, H., Saitoh, Y., Koizumi, K., Aozuka, Y., Sekine, K., Yamada, M., Saiki, I. and Nishikawa, K. (2006). Aminopeptidase N (APN/CD13) is selectively expressed in vascular endothelial cells and plays multiple roles in angiogenesis. *Cancer Lett.* **243**, 135-143.

Furlanetto, R. W., Dey, B. R., Lopaczynski, W. and Nissley, S. P. (1997). 14-3-3 proteins interact with the insulin-like growth factor receptor but not the insulin receptor. *Biochem. J.* **327**, 765-771.

Gabison, E. E., Hoang-Xuan, T., Mauviel, A. and Menashi, S. (2005). EMMPRIN/CD147, an MMP modulator in cancer, development and tissue repair. *Biochimie* **87**, 361-368.

Garner, W. L. (1998). Epidermal regulation of dermal fibroblast activity. *Plast. Reconstr. Surg.* **102**, 135-139.

Ghaffari, A., Li, Y., Karami, A., Ghaffari, M., Tredget, E. E. and Ghahary, A. (2006). Fibroblast extracellular matrix gene expression in response to keratinocyte-releasable stratifin. *J. Cell. Biochem.* **98**, 383-393.

Ghahary, A., Karimi-Busheri, F., Marcoux, Y., Li, Y., Tredget, E. E., Taghi, K. R., Li, L., Zheng, J., Karami, A., Keller, B. O. et al. (2004). Keratinocyte-releasable stratifin functions as a potent collagenase-stimulating factor in fibroblasts. *J. Invest. Dermatol.* **122**, 1188-1197.

Giannelli, G., Falk-Marzillier, J., Schiraldi, O., Stetler-Stevenson, W. G. and Quaranta, V. (1997). Induction of cell migration by matrix metalloprotease-2 cleavage of laminin-5. *Science* **277**, 225-228.

Harrison, C. A., Gossiel, F., Bullock, A. J., Sun, T., Blumsohn, A. and Mac, N. S. (2006). Investigation of keratinocyte regulation of collagen I synthesis by dermal fibroblasts in a simple in vitro model. *Br. J. Dermatol.* **154**, 401-410.

Hermeking, H. (2003). The 14-3-3 cancer connection. *Nat. Rev. Cancer* **3**, 931-943.

Ichimura, E., Yamada, M., Nishikawa, K., Abe, F. and Nakajima, T. (2006). Immunohistochemical expression of aminopeptidase N (CD13) in human lung squamous cell carcinomas, with special reference to Bestatin adjuvant therapy. *Pathol. Int.* **56**, 296-300.

Katz, A. B. and Taichman, L. B. (1999). A partial catalog of proteins secreted by epidermal keratinocytes in culture. *J. Invest. Dermatol.* **112**, 818-821.

Keller, M., Ruegg, A., Werner, S. and Beer, H. D. (2008). Active caspase-1 is a regulator of unconventional protein secretion. *Cell* **132**, 818-831.

Kessenbrock, K., Plaks, V. and Werb, Z. (2010). Matrix metalloproteinases: regulators of the tumor microenvironment. *Cell* **141**, 52-67.

Kilani, R. T., Maksymowych, W. P., Aitken, A., Boire, G., St-Pierre, Y., Li, Y. and Ghahary, A. (2007). Detection of high levels of 2 specific isoforms of 14-3-3 proteins in synovial fluid from patients with joint inflammation. *J. Rheumatol.* **34**, 1650-1657.

Kobayashi, R., Deavers, M., Patenia, R., Rice-Stitt, T., Halbe, J., Gallardo, S. and Freedman, R. S. (2009). 14-3-3 zeta protein secreted by tumor associated monocytes/macrophages from ascites of epithelial ovarian cancer patients. *Cancer Immunol. Immunother.* **58**, 247-258.

Lai A, Ghaffari A and Ghahary A. (2010). Inhibitory effect of anti-aminopeptidase N/CD13 antibodies on fibroblast migration. *Mol. Cell Biochem.* (Epub ahead of print) PMID: 20589526.

Lam, E., Kilani, R. T., Li, Y., Tredget, E. E. and Ghahary, A. (2005). Stratifin-induced matrix metalloproteinase-1 in fibroblast is mediated by c-fos and p38 mitogen-activated protein kinase activation. *J. Invest. Dermatol.* **125**, 230-238.

Lee, J. P., Jalili, R. B., Tredget, E. E., Demare, J. R. and Ghahary, A. (2005). Antifibrogenic effects of liposome-encapsulated IFN-alpha2b cream on skin wounds in a fibrotic rabbit ear model. *J. Interferon. Cytokine Res.* **25**, 627-631.

Leffers, H., Madsen, P., Rasmussen, H. H., Honore, B., Andersen, A. H., Walbum, E., Vandekerckhove, J. and Celis, J. E. (1993). Molecular cloning and expression of the transformation sensitive epithelial marker stratifin. A member of a protein family that has been involved in the protein kinase C signalling pathway. *J. Mol. Biol.* **231**, 982-998.

Li, Y., Tredget, E. E., Ghaffari, A., Lin, X., Kilani, R. T. and Ghahary, A. (2006). Local expression of indoleamine 2,3-dioxygenase protects engraftment of xenogeneic skin substitute. *J. Invest. Dermatol.* **126**, 128-136.

Li, Y., Lin, X., Kilani, R. T., Jones, J. C. and Ghahary, A. (2007). 14-3-3 sigma isoform interacts with the cytoplasmic domain of the transmembrane BP180 in keratinocytes. *J. Cell Physiol.* **212**, 675-681.

Luan, Y. and Xu, W. (2007). The structure and main functions of aminopeptidase N. *Curr. Med. Chem.* **14**, 639-647.

Machesney, M., Tidman, N., Waseem, A., Kirby, L. and Leigh, I. (1998). Activated keratinocytes in the epidermis of hypertrophic scars. *Am. J. Pathol.* **152**, 1133-1141.

Mackay, A. R., Ballin, M., Pelina, M. D., Farina, A. R., Nason, A. M., Hartzler, J. L. and Thorgeirsson, U. P. (1992). Effect of phorbol ester and cytokines on matrix metalloproteinase and tissue inhibitor of metalloproteinase expression in tumor and normal cell lines. *Invasion Metastasis* **12**, 168-184.

McGonigle, S., Beall, M. J., Feeney, E. L. and Pearce, E. J. (2001). Conserved role for 14-3-3epsilon downstream of type I TGFbeta receptors. *FEBS Lett.* **490**, 65-69.

Mina-Osorio, P. (2008). The moonlighting enzyme CD13: old and new functions to target. *Trends Mol. Med.* **14**, 361-371.

Mina-Osorio, P., Shapiro, L. H. and Ortega, E. (2006). CD13 in cell adhesion: aminopeptidase N (CD13) mediates homotypic aggregation of monocytic cells. *J. Leukocyte Biol.* **79**, 719-730.

Mori, L., Bellini, A., Stacey, M. A., Schmidt, M. and Mattoli, S. (2005). Fibrocytes contribute to the myofibroblast population in wounded skin and originate from the bone marrow. *Exp. Cell Res.* **304**, 81-90.

Morris, D. E., Wu, L., Zhao, L. L., Bolton, L., Roth, S. I., Ladin, D. A. and Mustoe, T. A. (1997). Acute and chronic animal models for excessive dermal scarring: quantitative studies. *Plast. Reconstr. Surg.* **100**, 674-681.

Mueller, M. M. and Fusenig, N. E. (2004). Friends or foes-bipolar effects of the tumour stroma in cancer. *Nat. Rev. Cancer* **4**, 839-849.

Nagase, H. and Woessner, J. F., Jr (1999). Matrix metalloproteinases. *J. Biol. Chem.* **274**, 21491-21494.

Nagase, H., Visse, R. and Murphy, G. (2006). Structure and function of matrix metalloproteinases and TIMPs. *Cardiovasc. Res.* **69**, 562-573.

Nickel, W. (2007). Unconventional secretion: an extracellular trap for export of fibroblast growth factor 2. *J. Cell Sci.* **120**, 2295-2299.

Niessen, F. B., Andriessen, M. P., Schalkwijk, J., Visser, L. and Timens, W. (2001). Keratinocyte-derived growth factors play a role in the formation of hypertrophic scars. *J. Pathol.* **194**, 207-216.

Nomura, R., Kiyota, A., Suzaki, E., Kataoka, K., Ohe, Y., Miyamoto, K., Senda, T. and Fujimoto, T. (2004). Human coronavirus 229E binds to CD13 in rafts and enters the cell through caveolae. *J. Virol.* **78**, 8701-8708.

Oksvold, M. P., Huitfeldt, H. S. and Langdon, W. Y. (2004). Identification of 14-3-3zeta as an EGF receptor interacting protein. *FEBS Lett.* **569**, 207-210.

Overall, C. M. and Lopez-Otin, C. (2002). Strategies for MMP inhibition in cancer: innovations for the post-trial era. *Nat. Rev. Cancer* **2**, 657-672.

Pilcher, B. K., Dumin, J. A., Sudbeck, B. D., Krane, S. M., Welgus, H. G., Parks, W. C. (1997). The activity of collagenase-1 is required for keratinocyte migration on a type I collagen matrix. *J. Cell Biol.* **137**, 1445-1457.

Pirilä, E., Sharabi, A., Salo, T., Quaranta, V., Tu, H., Heljasvaara, R., Koshikawa, N,. Sorsa, T. and Maisi, P. (2003). Matrix metalloproteinases process the laminin-5 γ2-chain and regulate epithelial cell migration. *Biochem. Biophys. Res. Commun.* **303**, 1012-1017.

Pozuelo, R. M., Geraghty, K. M., Wong, B. H., Wood, N. T., Campbell, D. G., Morrice, N. and Mackintosh, C. (2004). 14-3-3-affinity purification of over 200 human phosphoproteins reveals new links to regulation of cellular metabolism, proliferation and trafficking. *Biochem. J.* **379**, 395-408.

Proost, P., Mortier, A., Loos, T., Vandercappellen, J., Gouwy, M., Ronsse, I., Schutyser, E., Put, W., Parmentier, M., Struyf, S. et al. (2007). Proteolytic processing of CXCL11 by APN/CD13/aminopeptidase N impairs CXCR3 and CXCR7 binding and signaling and reduces lymphocyte and endothelial cell migration. *Blood* **110**, 37-44.

Radisky, D. C. and Bissell, M. J. (2004). Cancer. Respect thy neighbor! *Science* **303**, 775-777.

Raynaud, F., Bauvois, B., Gerbaud, P. and Evain-Brion, D. (1992). Characterization of specific proteases associated with the surface of human skin fibroblasts, and their modulation in pathology. *J. Cell Physiol.* **151**, 378-385.

Redegeld, F. A., Smith, P., Apasov, S. and Sitkovsky, M. V. (1997). Phosphorylation of T-lymphocyte plasma membrane-associated proteins by ectoprotein kinases: implications for a possible role for ectophosphorylation in T-cell effector functions. *Biochim. Biophys. Acta* **1328**, 151-165.

Riemann, D., Kehlen, A. and Langner, J. (1999). CD13-not just a marker in leukemia typing. *Immunol. Today* **20**, 83-88.

Rodriguez, D., Morrison, C. J. and Overall, C. M. (2010). Matrix metalloproteinases: What do they not do? New substrates and biological roles identified by murine models and proteomics. *Biochim. Biophys. Acta* **1803**, 39-54.

Saiki, I., Fujii, H., Yoneda, J., Abe, F., Nakajima, M., Tsuruo, T. and Azuma, I. (1993). Role of aminopeptidase N (CD13) in tumor-cell invasion and extracellular matrix degradation. *Int. J. Cancer* **54**, 137-143.

Santos, A. N., Langner, J., Herrmann, M. and Riemann, D. (2000). Aminopeptidase N/CD13 is directly linked to signal transduction pathways in monocytes. *Cell Immunol.* **201**, 22-32.

Satoh, J., Kurohara, K., Yukitake, M. and Kuroda, Y. (1999). The 14-3-3 protein detectable in the cerebrospinal fluid of patients with prion-unrelated neurological diseases is expressed constitutively in neurons and glial cells in culture. *Eur. Neurol.* **41**, 216-225.

Sorrell, J. M., Baber, M. A., Brinon, L., Carrino, D. A., Seavolt, M., Asselineau, D. and Caplan, A. I. (2003). Production of a monoclonal antibody, DF-5, that identifies cells at the epithelial-mesenchymal interface in normal human skin. APN/CD13 is an epithelial-mesenchymal marker in skin. *Exp. Dermatol.* **12**, 315-323.

Strochlic, L., Cartaud, A., Mejat, A., Grailhe, R., Schaeffer, L., Changeux, J. P. and Cartaud, J. (2004). 14-3-3 gamma associates with muscle specific kinase and regulates synaptic gene transcription at vertebrate neuromuscular synapse. *Proc. Natl. Acad. Sci. USA* **101**, 18189-18194.

Terauchi, M., Kajiyama, H., Shibata, K., Ino, K., Nawa, A., Mizutani, S. and Kikkawa, F. (2007). Inhibition of APN/CD13 leads to suppressed progressive potential in ovarian carcinoma cells. *BMC Cancer* **27**, 140.

Toriseva, M. and Kahari, V. M. (2009). Proteinases in cutaneous wound healing. *Cell. Mol. Life Sci.* **66**, 203-224.

Turner, M. D., Handel, S. E., Wilde, C. J. and Burgoyne, R. D. (1993). Differential effect of brefeldin A on phosphorylation of the caseins in lactating mouse mammary epithelial cells. *J. Cell Sci.* **106**, 1221-1226.

Tzivion, G., Luo, Z. and Avruch, J. (1998). A dimeric 14-3-3 protein is an essential cofactor for Raf kinase activity. *Nature* **394**, 88-92.

Tzivion, G., Shen, Y. H. and Zhu, J. (2001). 14-3-3 proteins; bringing new definitions to scaffolding. *Oncogene* **20**, 6331-6338.

Uludag, H., D'Augusta, D., Palmer, R., Timony, G. and Wozney, J. (1999). Characterization of rhBMP-2 pharmacokinetics implanted with biomaterial carriers in the rat ectopic model. *J. Biomed. Mater. Res.* **46**, 193-202.

Wang, B., Yang, H., Liu, Y. C., Jelinek, T., Zhang, L., Ruoslahti, E. and Fu, H. (1999). Isolation of high-affinity peptide antagonists of 14-3-3 proteins by phage display. *Biochemistry* **38**, 12499-12504.

Waterman, M. J., Stavridi, E. S., Waterman, J. L. and Halazonetis, T. D. (1998). ATM-dependent activation of p53 involves dephosphorylation and association with 14-3-3 proteins. *Nat. Genet.* **19**, 175-178.

Yaffe, M. B. (2002). How do 14-3-3 proteins work?- Gatekeeper phosphorylation and the molecular anvil hypothesis. *FEBS lett.* **513**, 53-57.

Yaffe, M. B., Rittinger, K., Volinia, S., Caron, P. R., Aitken, A., Leffers, H., Gamblin, S. J., Smerdon, S. J. and Cantley, L. C. (1997). The structural basis for 14-3-3:phosphopeptide binding specificity. *Cell* **91**, 961-971.